

Glu-Trp-ONa or its acylated analogue (R-Glu-Trp-ONa) administration enhances the wound healing in the model of chronic skin wounds in rabbits

Maxim A Shevtsov^{1,2}

Larisa V Smagina¹

Tatiana A Kudriavtceva³

Sergey V Petlenko⁴

Irina V Voronkina¹

¹Institute of Cytology of the Russian Academy of Sciences (RAS), St Petersburg, Russia; ²IP Pavlov State Medical University of St Petersburg, St Petersburg, Russia;

³Institute of Experimental Medicine of the North-West Branch of the Russian Academy of Medical Sciences (IEM NWB RAMS), St Petersburg, Russia; ⁴Military Medical Academy, St Petersburg, Russia

Abstract: The management of chronic skin wounds represents a major therapeutic challenge. The synthesized dipeptide (Glu-Trp-ONa) and its acylated analogue (R-Glu-Trp-ONa) were assessed in the model of nonhealing dermal wounds in rabbits in relation to their healing properties in wound closure. Following wound modeling, the rabbits received a course of intraperitoneal injections of Glu-Trp-ONa or R-Glu-Trp-ONa. Phosphate-buffered saline and Solcoseryl® were applied as negative and positive control agents, respectively. An injection of Glu-Trp-ONa and R-Glu-Trp-ONa decreased the period of wound healing in animals in comparison to the control and Solcoseryl-treated groups. Acylation of Glu-Trp-ONa proved to be beneficial as related to the healing properties of the dipeptide. Subsequent zymography analyses showed that the applied peptides decreased the proteolytic activity of matrix metalloproteinases MMP-9, MMP-8, and MMP-2 in the early inflammatory phase and reversely increased the activity of MMP-9, MMP-8, and MMP-1 in the remodeling phase. Histological analyses of the wound sections (hematoxylin–eosin, Mallory’s staining) confirmed the enhanced formation of granulation tissue and re-epithelialization in the experimental groups. By administering the peptides, wound closures increased significantly through the modulation of the MMPs’ activity, indicating their role in wound healing.

Keywords: chronic wound, matrix metalloproteinases, small peptides

Introduction

The management of chronic wounds has become a major therapeutic challenge with the increasing incidence of conditions such as diabetes, obesity, and vascular disorders.¹ Development of novel and effective approaches in wound care remains an area of intense research, and numerous modalities (eg, growth factors, biologic dressings, skin substitutes, regenerative materials, hydroconductive dressings, etc) have been proposed.² Among bioactive therapies, the application of peptides could offer an innovative solution in wound repair.

Several updated peptides have been proposed for regenerative medicines (eg, thymosin β 4 [T β 4], collagen peptides, laminin-derived peptides, cryptic peptides from bovine Achilles tendon collagen, platelet-derived peptides) including those that heal wounds.^{3–10} Thus, the small synthetic peptide IDR-1018, termed as an innate defense regulator, demonstrated anti-infective, anti-inflammatory, wound healing, and anti-biofilm activities.¹⁰ The in vivo activity of the IDR-1018 peptide clearly showed enhancement of wound healing and an ability to protect against *Staphylococcus aureus*.¹⁰ Another study suggested that the 19-amino-acid designer peptide SHAP1 possessed salt-resistant antimicrobial activities, and also proved to be beneficial in wound closure.⁷

Correspondence: Maxim A Shevtsov; Irina V Voronkina
Institute of Cytology of the Russian Academy of Sciences (RAS), Tikhoretsky Avenue 4, St Petersburg, 194064 Russia
Tel +7 812 297 1829
Fax +7 812 297 1834
Email shevtsov-max@mail.ru; voronirina@list.ru

Another class of peptides first described by Goldstein and White in 1966 that were derived from thymus (ie, thymosins) represents a promising approach in treatment of dermal wounds.^{11–13} In the study by Kim et al it was clearly demonstrated that intradermally administered T β 4 in a dermal burn wounds in vivo model in mice improved wound-healing markers such as wound closure, granulation, and vascularization.¹⁴ Moreover, the thymus derived peptide T β 4 clearly enhanced biomechanical properties of fractures in mice, proving its therapeutic potential.⁵ The therapeutic wound-healing effect of T β 4 was attributed to its ability to bind actin and promote cell migration, as well as the mobilization and differentiation of stem/progenitor cells, which contribute to tissue regeneration.¹⁵ In the study by Freeman et al an extracellular signaling pathway was identified where T β 4 increased cell surface ATP levels via ATP synthase, and showed the importance of the ATP-responsive P2X4 receptor for the thymosin-induced human umbilical vein endothelial cell migration.¹⁶ T β 4 and its sulfoxized form also significantly accelerated wound closure and increased the chemotaxis of C2C12 myoblastic cells in adult mice, thus proving the chemoattractant activity of T β 4.¹⁷

Such properties of T β 4 provided the scientific rationale for the study evaluating the tissue repairing potential of chemically modified peptides. For the assessment of wound-healing efficacy of peptides, we implicated the thymus derived dipeptide (L-Glu-L-Trp) that had previously demonstrated tissue regenerative activity.^{18,19} The presence of a glutamic acid residue at the N-terminus of the peptide leads in the physiological conditions to the formation of its pyroglutamate derivate that reduces the biological activity of Glu-Trp-ONa. To increase the proteolytic stability, we synthesized acylated dipeptide analog (R-Glu-Trp-ONa) that was further analyzed in relation to its wound-healing properties in a model of chronic wounds in rabbits.

Materials and methods

Glu-Trp-ONa and R-Glu-Trp-ONa

Glu-Trp-ONa and its acylated lipophilic analogue (R-Glu-Trp-ONa) were provided by the Medical Biological Research and Development Centre “Cytomed” (St Petersburg, Russia). Lipopolysaccharide was depleted with the help of the Polymyxin B-Agarose endotoxin removing gel (Sigma-Aldrich Co., St Louis, MO, USA). The quantitation of endotoxin was performed using the *Limulus* amoebocyte lysate assay (E-toxate LAL kit; Sigma-Aldrich Co.). The resulting endotoxin content was below 0.1 EU/mg. For negative control, phosphate-buffered saline (PBS) was applied. For positive

control, Solcoseryl® containing dialysate ultrafiltrate derived from calf blood was implicated (MEDA Pharmaceuticals Switzerland GmbH, Wangen-Brüttisellen, Switzerland).

Study design

All experimental studies were conducted in healthy animals. Following modeling of the chronic nonhealing dermal wounds, the rabbits were randomly assigned to six groups (three animals each) as follows: group 1 received an intraperitoneal injection of PBS solution (5.0 mL per injection, total of 21 injections); group 2 received intraperitoneal administration of Glu-Trp-ONa (0.04 mg/kg, 5.0 mL per injection, total of 21 injections); groups 3, 4, and 5 were administered with lipophilic analogues at 0.04, 0.2, and 1.0 mg/kg, respectively; group 6 was treated with Solcoseryl at 0.8 mL/kg and was regarded as positive control. All injections started on the first day following operation and were performed daily for 21 days. For analysis of the metalloproteinases (MMP-1, MMP-2, MMP-8, and MMP-9) activity during the epithelization process, wound fluid was collected on the third, sixth, ninth, 12th, 15th, 18th, 21th, and 24th day following operation in animals from all six groups. MMP-9 and -8 were selected for analysis as these proteinases are predominantly produced by the macrophages and neutrophil cells at the early inflammatory stage. MMP-2 and -1 are produced by fibroblasts during the proliferative and remodeling phases of wound healing. On the 24th day, all rabbits were sacrificed, and the wounds were debulked and assessed with the help of histological examination.

Animals and anesthesia

Eighteen male New Zealand rabbits (Rappolovo Russian Academy of Medical Sciences, St Petersburg, Russia) weighing 3.8–3.9 kg were used for this study. All treatments were conducted in accordance with the US Department of Health and Human Services Guide for the Care and Use of Laboratory Animals (1996). All experimental protocols were approved, and the procedures followed were in accordance with the ethical standards of the IP Pavlov State Medical University of St Petersburg (St Petersburg, Russia). For anesthesia, we used intravenous injections of ketamine (10–50 mg/kg) and xylazine (1–3 mg/kg) mixture, which were administered directly into the marginal ear vein after placement of a catheter. A light sedative agent – fentanyl/droperidol (0.2 mg/kg, intramuscular injection [IM]) – was used prior to anesthesia to avoid stress in the rabbits. For tranquilization and muscle relaxation during intubation of the rabbits, benzodiazepine (diazepam, 1 mg/kg,

intravenously) was used. During surgery, heart rate (at 130–325 bpm) and respiratory rate (at 32–60 per minute) were monitored, as well as blood pressure (at 90–130/90–60 mmHg) and body temperature (at level 38.5°C–39.6°C).

Modeling of the chronic nonhealing dermal wound

Following anesthesia in the paravertebral region, the rabbit's dorsal skin was shaved with electric clippers and cleansed with 10% povidone-iodine and 70% alcohol swabs before manipulation. Before making a dermal wound, the skin was marked with a round shaped film stencil, thus providing a uniform area for each wound. A circular shaped defect of the skin, subcutaneous tissue, and superficial fascia was created with a diameter of 22 mm, 3 cm lateral to the cervicothoracic vertebral column below the scapula. The edges of the skin flap were sutured to the edge of the silicone ring (inner diameter 20 mm, height 5 mm) so that the edge of the skin tightly attached to the underlying tissues (Figure 1). The wound was closed with Cosmopor adhesive sterile bandages (Hartman Paul AG, Heidenheim, Germany). All animals received analgesia with ketoprofen (1.0 mg/kg, IM, daily). Following the operation, none of the animals received any antibiotic therapy. Every 3 days under general anesthesia (ketamine [35–50 mg/kg] plus xylazine [5–10 mg/kg], IM), the ligation was performed.

During each dressing, we collected the wound exudation to assess the activity of MMPs. Samples of wound fluid were collected during each dressing by applying round sterile filter paper moistened with PBS (2 minutes exposure) (Figure 2). Thereafter, the filter was transferred to a sterile test tube that was immediately cooled on ice and stored at -70°C until analysis. Samples were taken from each wound

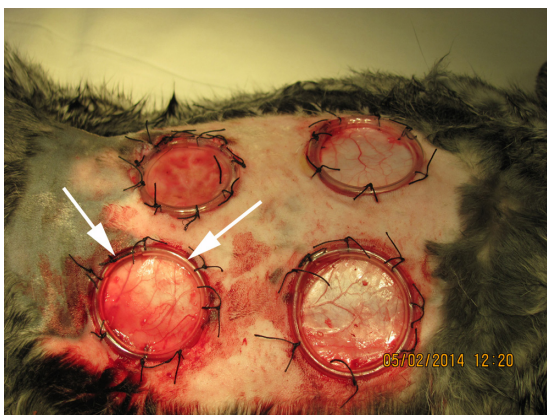


Figure 1 Macrophotography of the nonhealing dermal wounds in rabbits.
Note: White solid arrows point to the silicone ring.

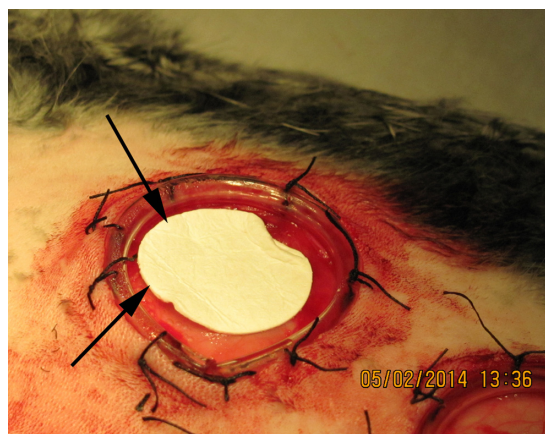


Figure 2 Collection of the wound fluid samples by sterile filter paper.

of each animal during the experimental study. Additionally, blood samples were obtained from each animal before the operation and during each dressing. At the end of the dressing, the wound was closed with a sterile bandage.

The area of wounds in experimental animals was measured every 3 days of the ligation with the help of the photofixation method. The obtained macrophotographs were processed using the image processing software ImageJ. The index of wound epithelization in terms of percentage of the original wound area was calculated. The average for three animals from each experimental group was calculated. Following removal of animals from the experiment, the wound was excised on the outer edge of the wound and fixed in 10% formalin for subsequent histological examination.

Zymography

To determine the activity of matrix metalloproteinases (MMP-1, MMP-2, MMP-8, and MMP-9) in the wounds of rabbits that received various treatments, wound fluid was sampled on the third, sixth, ninth, 12th, 15th, 18th, 21st, and 24th day following dermal wound modeling. MMP activity was determined by the zymography method described.²⁰ Gelatin and casein were used as substrates to evaluate the activity of gelatinases (MMP-2, MMP-9) and collagenases (MMP-1, MMP-8), respectively. Wound fluid samples were separated from debris by centrifugation, mixed with sample buffer without b-mercaptoethanol, and subjected to electrophoresis. A gel (10% acrylamide) contained 1.0 mg/mL gelatin or 0.5 mg/mL casein. Ten micrograms of protein per lane were loaded in gel. Protein content in probes was measured by Bradford protein assay. After electrophoresis, the gel was washed twice with 2.5% Triton X-100 for 30 minutes and then incubated in a buffer solution (50 mM Tris-HCl pH

7.6, 0.15 M NaCl, 10 mM CaCl₂, 0.05% Brij 35) for 12 hours. Then, the gel was stained with Coomassie Blue R-250 (0.25% Coomassie brilliant blue R-250 in 40% isopropanol for 2 hours) and, after destaining (destained with 7% acetic acid for 1 hour), the bands containing MMP were developed as nonstained bands. A medium conditioned by HT-1080 fibroblasts was used as a marker to determine MMP zones (obtained from Culture Collections of Institute of Cytology of the Russian Academy of Sciences [RAS], St Petersburg, Russia). For quantitative assay, gels were scanned and images were processed with QuantiScan 2.1 software. MMP activity, presented as arbitrary units, was taken in the program QuantiScan (the number of colored pixels according to band \times the intensity of color). The results of densitometry were presented as histograms.

Histological examination of the wound samples

Skin samples were placed into a 10% neutral-buffered formalin, switched to 70% ethanol after 24–48 hours, routinely processed, embedded in paraffin wax, and sectioned at 15 μ m. Serial sections were routinely stained with hematoxylin–eosin (H&E) as well as Masson's trichrome for collagen and Mallory's staining. Wound healing in H&E and Masson's trichrome-stained slides were semiquantitatively evaluated by an experienced pathologist with a Leica DM4000 B LED light microscope with attached digital camera (Leica Microsystems, Wetzlar, Germany). In brief, acute and chronic inflammation; amount and maturation of granulation tissue; collagen deposition; re-epithelialization; and neovascularization were assessed. Acute inflammation was defined by the presence of neutrophils, while chronic inflammation was characterized by lymphoplasmacytic and monocytic infiltrate.

Statistical analysis

The open source software package R version 2.15.2 was used for analysis.²¹ Nonparametric Mann–Whitney test was run for pairwise comparisons to determine if the group with the largest parameter was statistically significantly larger than all of the other groups. Statistical significance was determined at $P < 0.05$.

Results

Administration of the Glu-Trp-ONa and its acylated analogue significantly increased wound closure

Following modeling of the chronic nonhealing dermal wound, all animals received PBS, Solcoseryl, Glu-Trp-ONa,

or acylated analogue injections. None of the wounds exhibited signs of infection at the time of harvesting. All infusions were well tolerated by the rabbits and we did not observe any side-effects (ie, behavioral changes) throughout the period of observation. When we assessed the kinetics of wound healing in each group, we observed a statistically significant increase in the wound closure in the rabbits treated with Glu-Trp-ONa and its acylated analogue (Figure 3). The measurement of the wound area clearly demonstrated the wound closure in the treatment groups (Figure 4A). Thus, application of Glu-Trp-ONa resulted in significantly less wound area in comparison to the control PBS-treated animals, ie, 19.9 ± 4.4 mm² and 29.7 ± 5.0 mm², respectively, on the 24th day ($P < 0.05$). Administration of the acylated analogue (at 0.2 mg/kg) also resulted in elevated wound closure in comparison to the control animals, ie, 25.3 ± 5.2 mm² ($P < 0.05$). Furthermore, increasing the concentration of acylated analogue up to 1.0 mg/kg, which was equivalent to the dose of Glu-Trp-ONa injected, further enhanced the wound-healing process, resulting in a wound size of 19.3 ± 3.4 mm². This was statistically distinct in comparison with the Glu-Trp-ONa treated group. Implementation of Solcoseryl did not result in any significant wound healing, with a result of 39.2 ± 7.7 mm² on the 24th day.

Infusion of Glu-Trp-ONa and its acylated analogue decreased chronic inflammation, and elevated eosinophils and polyploid cells

At the end of the observation period, all animals were sacrificed, and wound tissue was debulked and assessed with the help of histological assay according to the histologic

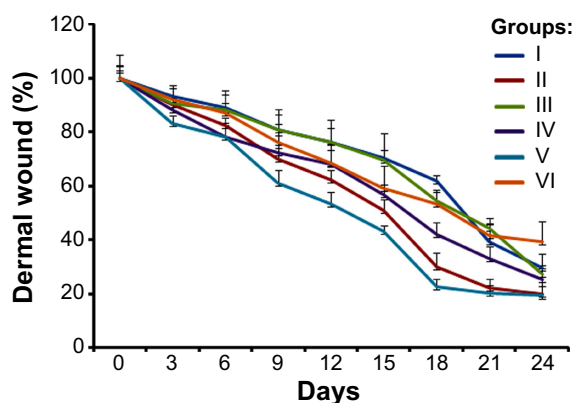


Figure 3 Kinetic analysis of wound healing in experimental animals.

Notes: Dermal wound (%) for control (phosphate-buffered saline-treated) group (group I); Glu-Trp-ONa-treated group (group II); animals treated with acylated analogue at 0.04, 0.2, and 1.0 mg/kg (groups III–V); and animals treated with Solcoseryl® (group VI). Data presented as means \pm standard error of three animals.

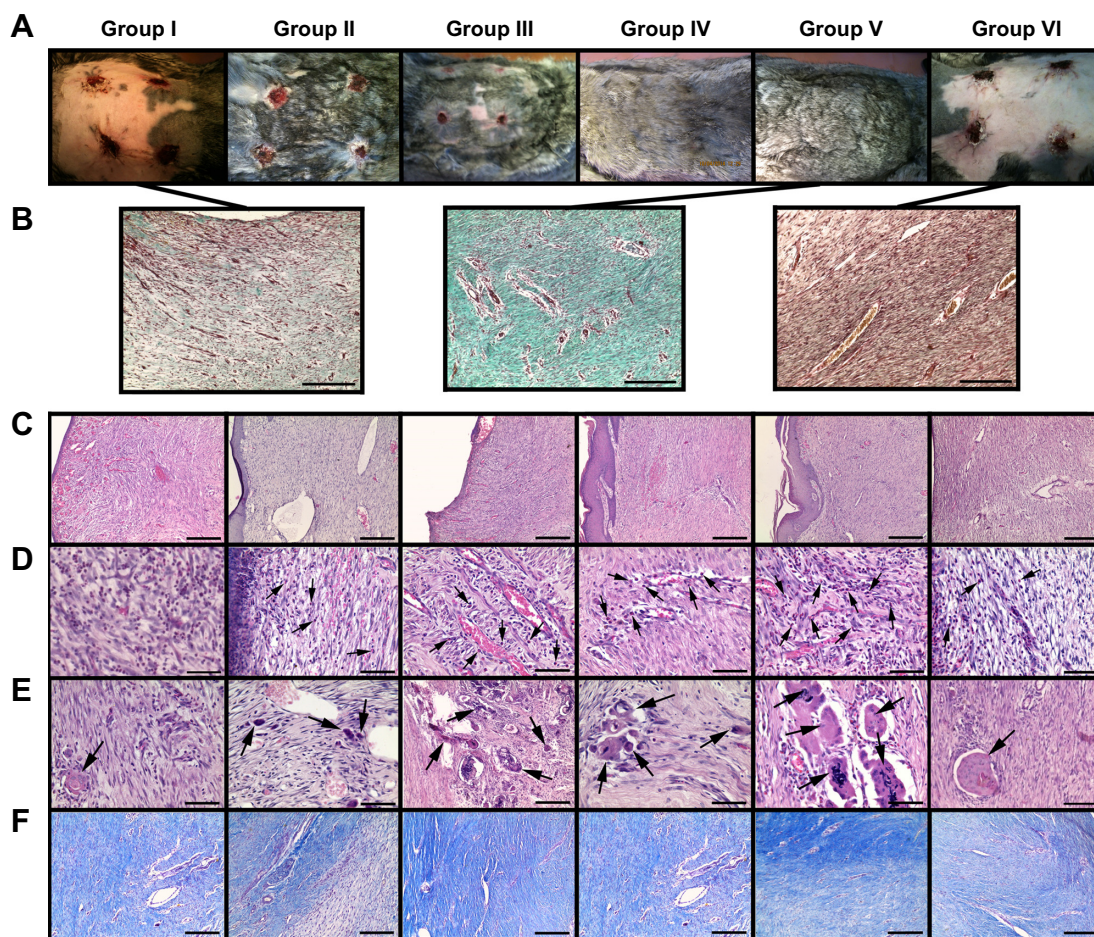


Figure 4 Analyses of the wound-healing processes in the experimental animals.

Notes: (A) Representative images of the nonhealing dermal wounds at the 21st day following operation in the rabbits for control (PBS-treated) group (group I); Glu-Trp-ONa-treated group (group II); animals treated with acylated analogue at 0.04, 0.2, and 1.0 mg/kg (groups III–V, respectively); and animals treated with Solcoseryl® (group VI). (B) Masson's trichrome staining for collagen. Scale bar: 200 μ m. (C) H&E staining of the wound sections. Representative images for the re-epithelialization process for animals from each study groups are depicted. Scale bar: 200 μ m. (D) H&E representative images of the wound depicting the eosinophilic infiltration (indicated by black solid arrows). Scale bar: 200 μ m. (E) Giant polykaryotic cells in the H&E sections (black arrows). Scale bar: 200 μ m. (F) Mallory's staining for granulation tissue for each treatment group. Scale bar: 250 μ m.

Abbreviations: H&E, hematoxylin–eosin; PBS, phosphate-buffered saline.

scoring system by Abramov et al with minor modification.²² In acute and chronic inflammation, amount and maturation of granulation tissue, eosinophilia, collagen deposition, re-epithelialization, and neovascularization were assessed independently and assigned a score of 0–3. According to this scheme, a score of 0 indicates none or no cells; 1, scant; 2, moderate; and 3, abundant. For re-epithelialization, a score of 0 represents none; 1, partial; 2, complete but immature or thin; and 3, complete. For neovascularization, a score of 0 indicates no vessels/high power field; 1, up to five vessels/high power field; 2, six to ten vessels/field of view; and 3, more than ten vessels/high power field. Wound margin borders in skin sections from all evaluated rabbits were clearly visible by light microscopy and were scored. Administration of Glu-Trp-ONa or its acylated analogue significantly elevated the re-epithelialization of the wound (Figure 4). At

the end of the observation period, we observed the nearly total closure of the wounds in the experimental groups, though in control animals we observed the presence of the chronic nonhealing wounds (Figure 4A). Thus, the thickness of the epidermis in the control and Solcoseryl-treated groups was 77.7 ± 14.5 and 80.9 ± 7.3 mm, respectively. Infusion of Glu-Trp-ONa increased the thickness of the epidermis by nearly twofold up to 135.1 ± 13.3 mm (Figure 4C). Acylated analogue also increased the thickness of the epidermis in a dose-dependent manner to 130.1 ± 11.1 , 142.4 ± 17.3 , and 154.8 ± 8.74 mm ($P < 0.001$). The thickness of the epidermis closely correlated with scores of re-epithelialization of the wound. Thus, the scores of re-epithelialization in groups I–VI were: 1.3 ± 0.14 , 2.0 ± 0.01 , 2.2 ± 0.11 , 2.3 ± 0.17 , 2.8 ± 0.04 , and 1.5 ± 0.15 , respectively. In the group of acylated analogue-treated rabbits (at 1.0 mg/kg),

we observed the highest parameters of maturation of the granulation tissue that was clearly demonstrated with the Mason trichrome (Figure 4B).

The scores of maturation of the granulation tissue were also elevated in Glu-Trp-ONa- and its acylated analogue-treated groups in comparison to control groups, namely 1.9 ± 0.04 , 2.0 ± 0.13 , 2.2 ± 0.11 , and 2.6 ± 0.01 ($P < 0.05$), corresponding to groups II–V. In control and Solcoseryl-treated groups, these scores were lower, namely 1.4 ± 0.15 and 1.34 ± 0.11 , respectively, corresponding to groups I and VI. Subsequent Mallory's staining demonstrated elevated maturation of the granulation tissue in Glu-Trp-ONa- and acylated analogue-treated groups (Figure 4F). Administration of Glu-Trp-ONa and acylated analogue also decreased the thickness of the leukocyte necrotic layer. Thus, in control and Solcoseryl-treated rabbits, the thickness of the necrotic layer was 214.7 ± 6.8 and 223.4 ± 11.2 mm, respectively. At the same time, the thickness of the necrotic layer for Glu-Trp-ONa and its analogue animals was 107.4 ± 8.9 , 109.7 ± 56.1 , 93.7 ± 6.4 , and 79.1 ± 11.3 mm, respectively, corresponding to groups II–V. Application of Glu-Trp-ONa and acylated analogue resulted in the increased eosinophilia in the histological sections in comparison to the PBS- or Solcoseryl-treated animals (Figure 4D). Thus, the index of eosinophilia for Glu-Trp-ONa and its analogue was 1.7 ± 0.14 , 2.2 ± 0.24 , 1.8 ± 0.13 , and 2.5 ± 0.15 , respectively, corresponding to groups II–V, while for control and Solcoseryl groups the index was 0.8 ± 0.15 and 2.3 ± 0.13 , respectively ($P < 0.05$). Analyses of the neovascularization score for Glu-Trp-ONa or analogue-treated animals demonstrated that indices were the same or slightly reduced compared to PBS- or Solcoseryl-treated controls. Intriguingly, we observed an increase in the multinuclear epithelioid cells in the wound tissue in the Glu-Trp-ONa and acylated analogue groups, namely 1.9 ± 0.3 , 1.5 ± 0.15 , 2.1 ± 0.23 , and 2.9 ± 0.15 , respectively, corresponding to groups II–V (Figure 4E). In the PBS- and Solcoseryl-treated groups, the indices were 0.9 ± 0.22 and 0.7 ± 0.23 , respectively.

Application of Glu-Trp-ONa and acylated analogue resulted in the modulation of the proteolytic activity of the matrix metalloproteinases

MMP activity was examined on such MMPs as gelatinase (MMP-2, MMP-9) and collagenase (MMP-1, MMP-8). Graphs of MMP activity during the wound-healing process are shown in Figure 5. The dynamics of MMP activity in all cases was statistically different from the dynamics of the normal wound-healing process (control). MMP activity

curves were smoothed when tested substances were administered in contrast to sharp activity peaks present in control groups. Administration of the tested substances resulted in a decrease of MMP activity levels that occurred earlier than with administration of PBS and Solcoseryl (Figure 5B). Application of Glu-Trp-ONa and its acylated analogue resulted in the decrease of MMP-2, MMP-8, and MMP-9 activity in the inflammatory phase, and activity of MMP-1, MMP-8, and MMP-9 were reversed in comparison to control animals in the remodulation phase of wound healing. Thus, following administration of the PBS in the first group of rabbits, the MMP-9 dynamics curve corresponded to normal wound healing, ie, a sharp activity increase during the third to sixth days after wound modeling and falling to zero further on during the healing process (Table 1). Infusion of Glu-Trp-ONa and acylated analogue significantly decreased MMP-9 activity, smoothing the increasing activity peaks until the 12th day, after which the MMP-9 activity was higher than for animals from the control group, leading to earlier termination of MMP-9 action (at 18–21 days). Administration of Glu-Trp-ONa decreased the MMP-9 activity relative to PBS and other tested substances. During the administration of PBS, the MMP-2 dynamics curve corresponded to normal wound healing, ie, activity increasing during the ninth to 12th days after wound modeling and falling to zero further on during the healing process (Table 2). Administration of Solcoseryl decreased the MMP-2 activity relative to PBS injection, smoothing the peaks of increased activity after 6 days, and after 15 days MMP activity was the same as for PBS. Administration of Glu-Trp-ONa decreased the MMP-2 activity and smoothed the peaks of activity, with MMP-2 activity decreasing to baseline faster (on the 21st day) than with other substances (on the 24th day). Infusion of acylated analogue at various concentrations also reduced the level of MMP-2 activity during the entire healing process relative to PBS. In these cases, the decrease of MMP-2 activity to the initial level occurred a little earlier. During the administration of PBS, the MMP-8 dynamics curve corresponded to normal wound healing, ie, activity increasing on the third day after wound modeling and falling to zero further on during the healing process (Table 3). Administration of Solcoseryl sharply decreased the MMP-8 activity from the third day until the end of the healing process. Administration of Glu-Trp-ONa also caused some reduction of MMP-8 activity and more rapid disappearance of MMP-8 activity in the inflammatory phase. Administration of acylated analogue reduced the level of MMP-8 activity during the third to 12th days, after which its activity dramatically increased in contrast to

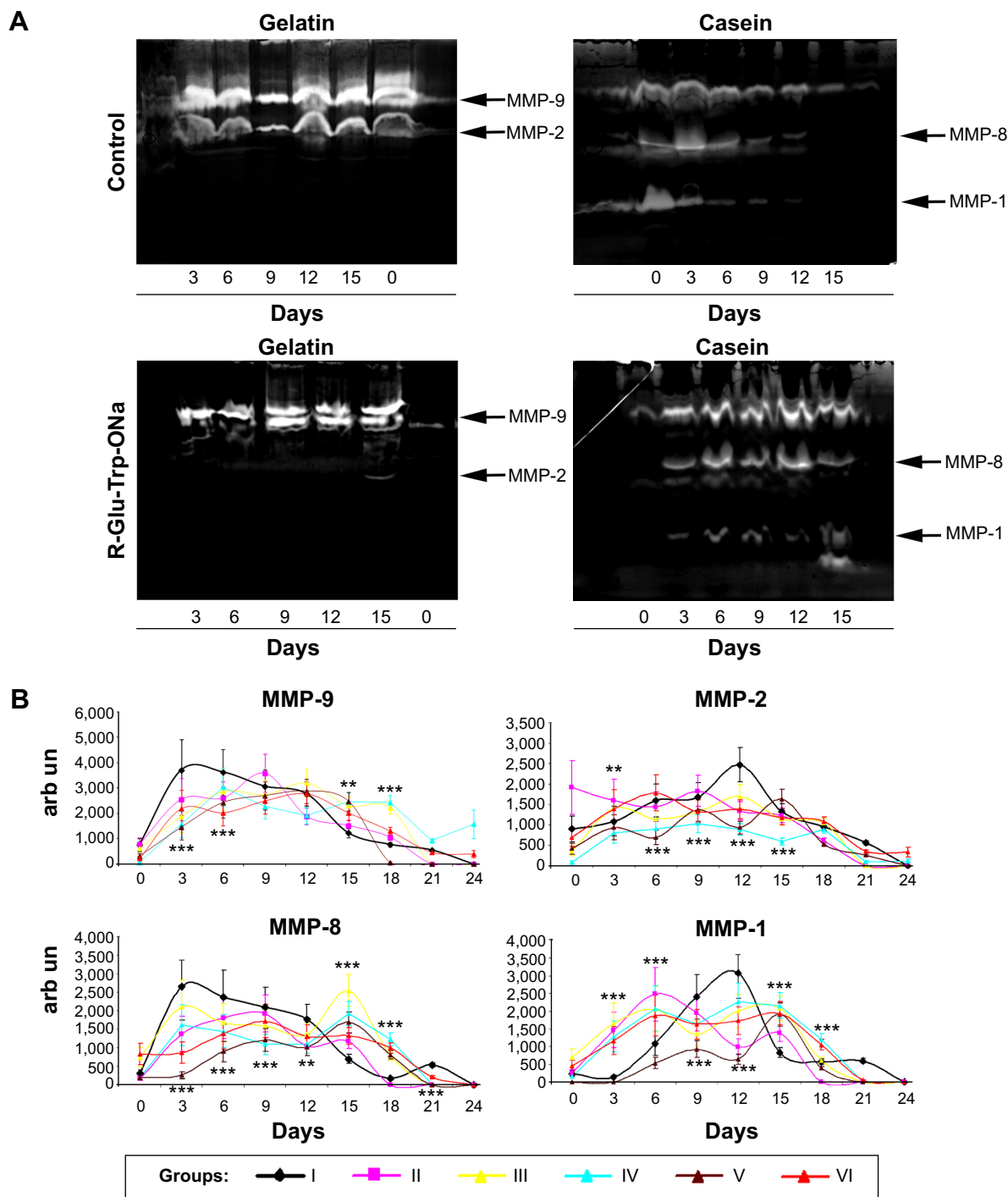


Figure 5 Zymography graphs for experimental studies.

Notes: (A) Representative zymograms for gelatin zymography (MMP-9, MMP-2) and casein zymography (MMP-8, MMP-1) of control and R-Glu-Trp-ONa- (1.0 mg/kg) treated animals. (B) MMP activity for MMP-1, MMP-2, MMP-8, and MMP-9 is presented in arbitrary units (arb un) for each treatment group. Wound fluid samples were collected every third day following operation (with the last sampling on the 24th day). The differences between the mean values in control and treatment groups were statistically significant at: *** $P < 0.001$; ** $P < 0.01$.

acylated analogue at 0.25 mg/kg during all healing process, relative to PBS. During administration of PBS, the MMP-1 dynamics curve corresponded to normal wound healing, ie, activity increasing during the tenth to 12th days after wound modeling with slow falling further on during the

healing process (Table 4). Administration of Solcoseryl, increased MMP-1 activity during the third to sixth days and reduced MMP-1 activity during the ninth to 15th days relative to PBS. Administration of Glu-Trp-ONa also resulted in increasing of MMP-1 activity during the third to sixth days,

Table 1 MMP-9 activity for all treatment groups

Activity of MMP-9						
Day	Group I	Group II	Group III	Group IV	Group V	Group VI
0	764.3±267.5	785.3±251.3	626.2±200.4	65.2±20.8	320.0±102.4	236.4±75.6
3	3,700.5±1,221.1 ***	2,550.7±841.7 ***	1,881.6±620.9 ***	1,564.8±516.4 ***	1,454.8±480.0 ***	2,192.4±723.5 ***
6	3,624.7±906.16 ***	2,604.5±651.12 ***	2,871.1±717.7 ***	3,039.3±759.8 ***	2,426.7±606.6 ***	2,030.1±507.5 ***
9	3,065.6±643.7	3,580.6±751.9	2,746.3±576.7	2,268.6±476.4	2,695.1±565.9	2,497.0±524.3
12	2,771.2±471.1	1,881.9±319.9	3,206.2±545.0	1,925.8±327.4	2,878.8±489.4	2,777.2±472.1
15	1,233.6±185.0 **	1,513.6±227.0 **	2,315.0±347.2 **	2,452.4±367.8 **	2,474.7±371.20 **	2,024.5±303.6 **
18	776.0±85.3 ***	1,051.5±115.6 ***	2,237.1±246.0 ***	2,431.0±267.4 ***	65.8±7.2 ***	1,313.9±144.5 ***
21	555.2±55.5	0	0	937.0±93.7	0	474.2±54.8
24	0	0	0	1,585.2±47.4	0	401.9±140.6

Notes: Activity of MMP-9 presented in arbitrary units for groups I–VI. The results are presented as mean ± standard error. ** $P < 0.01$. *** $P < 0.001$.

Table 2 MMP-2 activity for all treatment groups

Activity of MMP-2						
Day	Group I	Group II	Group III	Group IV	Group V	Group VI
0	895.9±313.5	1,918.4±652.2	361.6±122.9	83.4±28.36	412.5±140.2	697.6±237.17
3	1,088.1±359.0 **	1,593.8±525.9 **	1,396.6±460.8 **	813.8±268.5 **	934.3±308.3 **	1,389.6±458.5 **
6	1,602.1±400.52 ***	1,439.6±359.8 ***	1,152.3±288.0 ***	901.0±225.2 ***	698.5±174.6 ***	1,780.1±445.0 ***
9	1,678.9±352.5 ***	1,828.9±384.0 ***	1,329.7±279.2 ***	1,029.7±216.23 ***	1,374.9±288.7 ***	1,330.0±279.3 ***
12	2,469.8±419.8 ***	1,341.8±228.1 ***	1,691.4±287.53 ***	889.0±151.1 ***	929.5±158.0 ***	1,379.8±234.5 ***
15	1,321.4±198.2 ***	1,231.9±184.7 ***	1,152.2±172.8 ***	588.7±88.30 ***	1,625.2±243.7 ***	1,179.9±176.9 ***
18	959.0±105.4	606.9±66.7	1,042.7±114.6	894.2±98.3	529.1±58.2	1,078.0±118.5
21	564.1±56.4	0	0	103.3±10.3	256.3±25.6	346.8±34.6
24	0	0	0	117.4±41.1	0	334.5±117.0

Notes: Activity of MMP-2 presented in arbitrary units for groups I–VI. The results are presented as mean ± standard error. ** $P < 0.01$. *** $P < 0.001$.

Table 3 MMP-8 activity for all treatment groups

Activity of MMP-8						
Day	Group I	Group II	Group III	Group IV	Group V	Group VI
0	304.3±106.5	181.2±63.4	738.8±258.59	200.4±70.14	196.2±68.68	827.1±289.4
3	2,655.4±902.8 ***	1,372.9±466.8 ***	2,105.7±715.9 ***	1,609.8±547.33 ***	260.4±88.5 ***	859.9±292.3 ***
6	2,362.8±732.4 ***	1,808.2±560.5 ***	1,678.1±520.22 ***	1,448.2±448.9 ***	900.4±279.13 ***	1,383.7±428.9 ***
9	2,092.2±543.9 ***	1,915.6±498.0 ***	1,605.6±417.44 ***	1,088.1±282.9 ***	1,209.6±314.5 ***	1,717.4±446.5 ***
12	1,761.9±405.2 **	1,033.4±237.6 **	1,366.9±314.4 **	1,105.5±254.2 **	1,012.4±232.8 **	1,312.7±301.9 **
15	700.3±119.0 ***	1,179.1±200.4 ***	2,543.9±432.4 ***	1,917.9±326.0 ***	1,683.3±286.2 ***	1,320.8±224.5 ***
18	181.2±25.3 ***	0 ***	778.9±109.0 ***	1,233.7±172.7 ***	811.7±113.6 ***	991.1±138.7 ***
21	534.5±58.8 ***	0 ***	0 ***	0 ***	0 ***	218.2±24.0 ***
24	0	0	0	0	0	0

Notes: Activity of MMP-8 presented in arbitrary units for groups I–VI. The results are presented as mean ± standard error. ** $P < 0.01$. *** $P < 0.001$.

Table 4 MMP-I activity for all treatment groups

Activity of MMP-I						
Day	Group I	Group II	Group III	Group IV	Group V	Group VI
0	243.7±85.3	265.3±92.87	689.7±241.3	161.7±56.6	0	451.0±157.8
3	142.1±48.3 ***	1,464.8±498.0 ***	1,660.3±564.4 ***	1,277.8±434.44 ***	0 ***	1,162.5±395.2 ***
6	1,088.4±337.4 ***	2,474.2±767.0 ***	2,053.3±636.5 ***	2,078.1±644.2 ***	532.1±164.9 ***	1,877.1±581.9 ***
9	2,404.3±625.1 ***	1,954.7±508.2 ***	1,363.9±354.6 ***	1,631.3±424.1 ***	929.2±241.5 ***	1,634.1±424.8 ***
12	3,074.3±707.0 ***	992.1±228.1 ***	2,003.2±460.7 ***	2,256.9±519.1 ***	643.8±148.0 ***	1,735.5±399.1 ***
15	824.9±140.2 ***	1,388.0±235.9 ***	2,079.5±353.5 ***	2,150.8±365.6 ***	1,902.6±323.4 ***	1,939.7±329.7 ***
18	567.2±79.4 ***	0 ***	605.5±84.7 ***	1,193.4±167.0 ***	384.8±53.8 ***	1,046.1±146.4 ***
21	597.1±65.6	0	0	0	0	61.6±6.7
24	0	0	0	0	0	0

Notes: Activity of MMP-I presented in arbitrary units for groups I–VI. The results are presented as mean ± standard error. *** $P < 0.001$.

followed by more rapid disappearance of MMP-1 activity during the ninth to 15th days. Administration of acylated analogue at 0.5 and 1.0 mg/kg increased the level of MMP-1 activity during the third to ninth days, after which the activity level was lower than that for PBS. In the remodeling phase of wound healing, the MMP-1 activity was higher in rabbits treated with acylated analogue (with the highest activity at 1.0 mg/kg of acylated analogue) ($P < 0.001$).

Discussion

Several up-to-date novel therapeutic specialized strategies have been proposed for wound healing.^{23,24} In the current study we focused on the application of Glu-Trp-ONa and its modified analogue. Intraperitoneal administration of the peptides did not cause any behavioral changes in all treated animals. Moreover, we observed an increase in the wound closure processes (Figure 4A). Wound healing represents a complex and dynamic process that could be divided into three or four distinct phases. According to Gilmore, the wound-healing process occurs in three phases: inflammatory, fibroblastic, and maturation.²⁵ This process was also denoted in earlier versions as inflammatory, proliferative, and remodeling, and this is maintained by some authors.²⁶ Other authors divide the healing process into the four-phases concept that constitutes the hemostasis phase, the inflammatory phase, the proliferative phase, and the remodeling phase.²⁶ The inflammatory phase begins with the injury itself and continues over the course of several days. The next is the proliferative phase in which an extracellular matrix and network of cells is formed. The remodeling phase begins after 2–3 weeks. MMPs, via their ability to alter the activity of their protein

substrates, participate in regulating mechanisms in all of these repair processes.²⁷ As was shown in recent studies, the dysfunction of the MMPs in the extracellular matrix could play a role in the wound-healing process.^{28–32} Thus, in the study by Serra et al it was demonstrated that chronic venous ulcers in patients were associated with high levels of MMP-9 and neutrophil gelatinase-associated lipocalin.²⁸

In our study, we observed a modulation of the MMP activity following infusion of Glu-Trp-ONa or its acylated analogue (Figure 5). During the early inflammatory phase, there was a reduction of activity of MMP-9, MMP-8, and MMP-2 in comparison to control animals. At the same time, the level of MMP-1 activity was higher for Glu-Trp-ONa and acylated analogue than in control ($P < 0.001$). MMP-1 (collagenase-1) is present in wounds during the re-epithelialization process and its activity subsides when the wound closure is complete.^{33,34} As was demonstrated by Pilcher et al MMP-1 facilitates keratinocyte migration over the dermal matrix by lessening the affinity of collagen–integrin contacts.³⁵ MMP-9 (gelatinase B) was also shown to play a major role in re-epithelialization after injury, inducing the keratinocyte migration.³⁶ At the same time, as was shown by Liu et al the increased activity of MMP-9 correlated inversely with the wound-healing rates.³⁷ Apparently, Glu-Trp-ONa or acylated analogue decreased the levels of MMP-9 in the early phase, thus reducing its excessive proinflammatory activity.

On the contrary, during the remodeling phase, there was an increase of MMP-9, MMP-8, and MMP-1 activity, especially in the experimental group, with the highest activity for lipophilic analogue at 1.0 mg/kg (Figure 5). As was shown previously, MMP-9 is involved in remodeling of the

stroma and reformation of the basement membrane.³⁸ MMP-9 stimulated fibroblast contraction on the collagen gel.³⁹ Kobayashi et al suggested that the mechanism for MMP-9 regulation of contraction is through the generation of active TGF- β 1.³⁹ MMP-1 is involved in type I collagen maturation during wound closure.^{40,41} Moreover, in the study by Muller et al MMP-1 expression was associated with good wound healing.⁴² Secreted MMP-1 was required in the epidermis to facilitate re-epithelialization by remodeling the basement membrane, promoting cell elongation and actin cytoskeletal reorganization, and activating extracellular signal-regulated kinase signaling.⁴³ When the JNK pathway was ectopically activated to overexpress MMP-1, the rate of healing was accelerated in an MMP-1-dependent manner.⁴³

Expression of MMP-8 is important in cutaneous wound healing. Thus, the authors observed a significant delay in wound closure in MMP-8^{-/-} mice and altered inflammatory response in their wounds, with a delay of neutrophil infiltration and alterations in the TGF- β 1 signaling pathway.⁴⁴ Intriguingly, in MMP-8^{-/-} mice, the authors observed an increase in the expression of MMP-9, suggesting that both proteases might act coordinately in this process.⁴⁴ The increase in MMP-1, MMP-8, and MMP-9 corresponded to the elevation in the granulation tissue formation and re-epithelialization, as proved by the histological assay (Figure 4). Moreover, in the H&E staining sections, we found that Glu-Trp-ONa and acylated analogue induced formation of the polyploid epithelial cells (Figure 4E). It was recently shown by Losick et al that polyploidization is essential for mechanical wound stabilization and subsequent re-epithelialization.⁴⁵ On the 21st day following wound formation, we observed significant eosinophilia in wound sections (Figure 4D). As was demonstrated, the eosinophils could be the source of MMP-9.^{46,47} Song et al suggested that sustained presence of the eosinophils together with their production of TGF- α in the granulation layer of the healing wounds plays an important role in the organization of healing wounds.⁴⁸

Our study using Glu-Trp-ONa and its acylated analogue in treatment of chronic nonhealing wounds in rabbits represents an important step in the development of novel therapeutic strategies for achieving wound healing. Administered small synthetic peptides significantly increased the wound closure through modulation of MMPs' activity, indicating their role in wound resolution.

Acknowledgments

This work was supported by grants from the Russian Foundation for Basic Research (No 13-04-12027-ofi-m and No

12-04-00935). The authors thank Olga G Genbach, Tatyana V Zakoldaeva, Irina V Kononova, Yulia I Shevchuk, Dmitriy N Suslov, and Oleg V Galibin for assistance with animal experiments; Galina Y Yukina for histological analysis; and Aleksey V Kochetkov for chemical synthesis. The animal experiments were supported by a grant from the Russian Science Foundation (No 14-50-00068) and with financial support from the Federal Agency of Scientific Organizations, Russia.

Disclosure

The authors report no conflicts of interest in this work.

References

1. Park NJ, Allen L, Driver VR. Updating on understanding and managing chronic wound. *Dermatol Ther*. 2013;26(3):236–256.
2. Montfrans CV, Stok M, Geerkens M. Biology of chronic wounds and new treatment strategies. *Phlebology*. 2014;29(1 suppl):165–167.
3. Demidova-Rice TN, Wolf L, Deckenback J, Hamblin MR, Herman IM. Human platelet-rich plasma- and extracellular matrix-derived peptides promote impaired cutaneous wound healing in vivo. *PLoS One*. 2012;7(2):e32146.
4. Gonzalez-Curiel I, Trujillo V, Montoya-Rosales A, et al. 1,25-dihydroxyvitamin D3 induces LL-37 and HBD-2 production in keratinocytes from diabetic foot ulcers promoting wound healing: an in vitro model. *PLoS One*. 2014;9(10):e111355.
5. Brady RD, Grills BL, Schuijers JA, et al. Thymosin β 4 administration enhances fracture healing in mice. *J Orthop Res*. 2014;32(10):1277–1282.
6. Zhu X, Zhou X, Yi J, Tong J, Wu H, Fan L. Preparation and biological activity of quaternized carboxymethyl chitosan conjugated with collagen peptide. *Int J Biol Macromol*. 2014;70:300–305.
7. Jung Kim D, Lee YW, Park MK, et al. Efficacy of the designer antimicrobial peptide SHAP1 in wound healing and wound infection. *Amino Acids*. 2014;46(10):2333–2343.
8. Senyürek I, Kempf WE, Klein G, et al. Processing of laminin α chains generates peptides involved in wound healing and host defense. *J Innate Immun*. 2014;6(4):467–484.
9. Banerjee P, Mehta A, Shanthi C. Investigation into the cyto-protective and wound healing properties of cryptic peptides from bovine Achilles tendon collagen. *Chem Biol Interact*. 2014;211:1–10.
10. Mansour SC, de la Fuente-Núñez C, Hancock RE. Peptide IDR-1018: modulating the immune system and targeting bacterial biofilms to treat antibiotic-resistant bacterial infections. *J Pept Sci*. Epub 2014 Oct 31.
11. Goldstein AL, Badamchian M. Thymosins: chemistry and biological properties in health and disease. *Expert Opin Biol Ther*. 2004;4(4):559–573.
12. Hannappel E. Beta-Thymosins. *Ann N Y Acad Sci*. 2007;1112:21–37.
13. Philp D, Kleinman HK. Animal studies with thymosin beta, a multi-functional tissue repair and regeneration peptide. *Ann N Y Acad Sci*. 2010;1194:81–86.
14. Kim S, Kwon J. Thymosin beta 4 improves dermal burn wound healing via downregulation of receptor of advanced glycation end products in db/db mice. *Biochim Biophys Acta*. 2014;1840(12):3452–3459.
15. Goldstein AL, Hannappel E, Sosne G, Kleinman HK. Thymosin β 4: a multi-functional regenerative peptide. Basic properties and clinical applications. *Expert Opin Biol Ther*. 2012;12(1):37–51.
16. Freeman KW, Bowman BR, Zetter BR. Regenerative protein thymosin beta-4 is a novel regulator of purinergic signaling. *FASEB J*. 2011;25(3):907–915.
17. Tokura Y, Nakayama Y, Fukada S, et al. Muscle injury-induced thymosin β 4 acts as a chemoattractant for myoblasts. *J Biochem*. 2011;149(1):43–48.

18. Chalisova NI, Khavinson V, Nozdrachev AD. Modulating and protective effects of thymic peptides in lymphoid tissue culture. *Dokl Biol Sci.* 2001;379:316–318.
19. Khavinson VKh, Kuznik BI, Ryzhak GA. [Peptide bioregulators: the new class of geroprotectors. Message 2. Clinical studies results]. *Adv Gerontol.* 2013;26(1):20–37. Russian.
20. Oliver GW, Stetler-Stevenson WG, Kleiner DE. Zymography, casein zymography, and reverse zymography: activity assays for proteases and their inhibitors. In: Sterchi EE, Stöcker W, editors. *Proteolytic Enzymes: Tools and Targets.* Heidelberg: Springer Berlin; 1999:63–76.
21. The R Project for Statistical Computing [homepage on the Internet]. Available from: <http://www.r-project.org>. Accessed March 12, 2015.
22. Abramov Y, Golden B, Sullivan M, et al. Histologic characterization of vaginal vs abdominal surgical wound healing in a rabbit model. *Wound Repair Regen.* 2007;15(1):80–86.
23. Alexander JW, Supp DM. Role of Arginine and Omega-3 Fatty Acids in Wound Healing and Infection. *Adv Wound Care (New Rochelle).* 2014;3(11):682–690.
24. Zielins ER, Atashroo DA, Maan ZN, et al. Wound healing: an update. *Regen Med.* 2014;9(6):817–830.
25. Gilmore MA. Phases of wound healing. *Dimens Oncol Nurs.* 1991; 5(3):32–34.
26. Maxson S, Lopez EA, Yoo D, Danilkovitch-Miagkova A, Leroux MA. Concise review: role of mesenchymal stem cells in wound repair. *Stem Cells Transl Med.* 2012;1(2):142–149.
27. Gill SE, Parks WC. Metalloproteinases and their inhibitors: regulators of wound healing. *Int J Biochem Cell Biol.* 2008;40(6–7):1334–1347.
28. Serra R, Buffone G, Falcone D, et al. Chronic venous leg ulcers are associated with high levels of metalloproteinases-9 and neutrophil gelatinase-associated lipocalin. *Wound Repair Regen.* 2013;21(3):395–401.
29. Serra R, Gallelli L, Buffone G, et al. Doxycycline speeds up healing of chronic venous ulcers. *Int Wound J.* Epub 2013 Apr 5.
30. Amato B, Coretti G, Compagna R, et al. Role of matrix metalloproteinases in non-healing venous ulcers. *Int Wound J.* Epub 2013 Oct 24.
31. Serra R, Grande R, Butrico L, et al. Effects of a new nutraceutical substance on clinical and molecular parameters in patients with chronic venous ulceration. *Int Wound J.* Epub 2014 Feb 25.
32. Serra R, Gallelli L, Conti A, et al. The effects of sulodexide on both clinical and molecular parameters in patients with mixed arterial and venous ulcers of lower limbs. *Drug Des Devel Ther.* 2014;8:519–527.
33. Saarialho-Kere UK, Vaalamo M, Airola K, Niemi KM, Oikarinen AI, Parks WC. Interstitial collagenase is expressed by keratinocytes that are actively involved in reepithelialization in blistering skin disease. *J Invest Dermatol.* 1995;104(6):982–988.
34. Inoue M, Kratz G, Haegerstrand A, Ståhle-Bäckdahl M. Collagenase expression is rapidly induced in wound-edge keratinocytes after acute injury in human skin, persists during healing, and stops at reepithelialization. *J Invest Dermatol.* 1995;104(4):479–483.
35. Pilcher BK, Dumin JA, Sudbeck BD, Krane SM, Welgus HG, Parks WC. The activity of collagenase-1 is required for keratinocyte migration on a type I collagen matrix. *J Cell Biol.* 1997;137(6):1445–1457.
36. McCawley LJ, O'Brien P, Hudson LG. Epidermal growth factor (EGF)- and scatter factor/hepatocyte growth factor (SF/HGF)-mediated keratinocyte migration is coincident with induction of matrix metalloproteinase (MMP)-9. *J Cell Physiol.* 1998;176(2):255–265.
37. Liu Y, Min D, Bolton T, et al. Increased matrix metalloproteinase-9 predicts poor wound healing in diabetic foot ulcers. *Diabetes Care.* 2009;32(1):117–119.
38. Mulholland B, Tuft SJ, Khaw PT. Matrix metalloproteinase distribution during early corneal wound healing. *Eye (Lond).* 2005;19(5):584–588.
39. Kobayashi T, Kim H, Liu X, et al. Matrix metalloproteinase-9 activates TGF- β and stimulates fibroblast contraction of collagen gels. *Am J Physiol Lung Cell Mol Physiol.* 2014;306(11):L1006–L1015.
40. Pilcher BK, Sudbeck BD, Dumin JA, Welgus HG, Parks WC. Collagenase-1 and collagen in epidermal repair. *Arch Dermatol Res.* 1998;290 Suppl:S37–S46.
41. Shin MK, Lee JW, Kim YI, Kim YO, Seok H, Kim NI. The effects of platelet-rich clot releasate on the expression of MMP-1 and type I collagen in human adult dermal fibroblasts: PRP is a stronger MMP-1 stimulator. *Mol Biol Rep.* 2014;41(1):3–8.
42. Muller M, Trocme C, Lardy B, Morel F, Halimi S, Benhamou PY. Matrix metalloproteinases and diabetic foot ulcers: the ratio of MMP-1 to TIMP-1 is a predictor of wound healing. *Diabet Med.* 2008;25(4):419–426.
43. Stevens LJ, Page-McCaw A. A secreted MMP is required for reepithelialization during wound healing. *Mol Biol Cell.* 2012;23(6): 1068–1079.
44. Gutiérrez-Fernández A, Inada M, Balbín M, et al. Increased inflammation delays wound healing in mice deficient in collagenase-2 (MMP-8). *FASEB J.* 2007;21(10):2580–2591.
45. Losick VP, Fox DT, Spradling AC. Polyploidization and cell fusion contribute to wound healing in the adult *Drosophila* epithelium. *Curr Biol.* 2013;23(22):2224–2232.
46. Ohno I, Ohtani H, Nitta Y, et al. Eosinophils as a source of matrix metalloproteinase-9 in asthmatic airway inflammation. *Am J Respir Cell Mol Biol.* 1997;16(3):212–219.
47. Kelly EA, Liu LY, Esnault S, Quinchia Johnson BH, Jarjour NN. Potent synergistic effect of IL-3 and TNF on matrix metalloproteinase 9 generation by human eosinophils. *Cytokine.* 2012;58(2):199–206.
48. Song BZ, Donoff RB, Tsuji T, Todd R, Gallagher GT, Wong DT. Identification of rabbit eosinophils and heterophils in cutaneous healing wounds. *Histochem J.* 1993;25(10):762–771.

Drug Design, Development and Therapy

Publish your work in this journal

Drug Design, Development and Therapy is an international, peer-reviewed open-access journal that spans the spectrum of drug design and development through to clinical applications. Clinical outcomes, patient safety, and programs for the development and effective, safe, and sustained use of medicines are a feature of the journal, which

Submit your manuscript here: <http://www.dovepress.com/drug-design-development-and-therapy-journal>

Dovepress

has also been accepted for indexing on PubMed Central. The manuscript management system is completely online and includes a very quick and fair peer-review system, which is all easy to use. Visit <http://www.dovepress.com/testimonials.php> to read real quotes from published authors.